Robotics and Computer-Integrated Manufacturing ▮ (▮▮▮▮) ▮▮▮–▮▮▮

Contents lists available at SciVerse ScienceDirect

Robotics and Computer-Integrated Manufacturing

journal homepage: www.elsevier.com/locate/rcim

Optimization of process parameters for pulsed laser milling of micro-channels on AISI H13 tool steel

Daniel Teixidor [a], Inés Ferrer [a], Joaquim Ciurana [a,*], Tugrul Özel [b]

[a] Department of Mechanical Engineering and Industrial Construction, Universitat de Girona, Av. Lluis Santaló s/n, 17071 Girona, Spain
[b] Department of Industrial and Systems Engineering, RUTGERS (The State University of New Jersey), New Jersey, USA

ARTICLE INFO

Article history:
Received 15 July 2011
Received in revised form
15 May 2012
Accepted 25 May 2012

Keywords:
Process parameters optimization
Process parameters selection
Laser milling process

ABSTRACT

This paper focuses on understanding the influence of laser milling process parameters on the final geometrical and surface quality of micro-channel features fabricated on AISI H13 steel. Optimal selection of process parameters is highly critical for successful material removal and high dimensional and surface quality for micro-sized die/mold applications. A set of designed experiments is carried out in a pulsed Nd:YAG laser milling system using AISI H13 hardened tool steel as work material. Arrays of micro-channels have been fabricated using a range of process parameters such as scanning speed (SS), pulse intensity (PI), and pulse frequency (PF). The relation between process parameters and quality characteristics has been studied with experimental modeling. Multi-criteria decision making for material and process parameter selection for desired surface quality and dimensional accuracy is investigated using an evolutionary computation method based on particle swarm optimization (PSO).

1. Introduction

The micro-manufacturing processes are a growing area and have found widespread use in a variety of applications, such as biomedical devices, which represent a niche market, thereby creating a need to find alternative processes to manufacture these components with low cost, high accuracy and high quality surface finishing.

Laser-energy beam processing is widely used for cutting, drilling, scribing, marking, welding, sintering and heat treatment applications [1]. Computer numerically controlled machining systems based on laser beams, also called laser milling systems, have become commercially available in recent years. Further developments in pulsed laser techniques and systems have increased the applicability of laser milling technology in production systems. Hence, it has become a viable alternative to conventional methods for producing complex and micro-features on difficult-to-process materials and is being employed increasingly in industry because of its known advantages.

Laser milling can be applied to a wide range of materials (metals and non-metals, soft and difficult-to-machine) and allows the production of parts with complex shapes without expensive tooling. Compared with other conventional mechanical processes, laser machining (milling) is a non-contact material removal process that removes much less material, involves highly localized heat input to the workpiece, minimizes distortion, and offers no tool wear. Therefore, the process is not limited by constraints such as maximum tool force, buildup edge formation, or tool chatter. Laser milling is a relatively new machining process that removes material in a layer-by-layer fashion. It is an ablation procedure that causes the vaporization of material as a result of interaction between a laser beam and the workpiece being machined [2]. However, it is important to distinguish between the laser interaction with metals and with polymers. Whenever metals are used, the laser beam heats, melts and vaporizes the metal (metal sublimation), while in polymers the process is based on the rupture of molecular chains (laser ablation).

Many laser machining systems designed for material removal (laser milling) are based on pulsed Nd:YAG laser sources with characteristic pulse lengths in the nanosecond and microsecond range [3–5]. The ablation process, which takes place within the pulse duration, sublimates the metal (melting and vaporization phases). There is enough time for a thermal wave to propagate into the material. Evaporation occurs from the liquid state of the material. The molten material is partially ejected from the cavity by the vapor and plasma pressure, but a portion of it remains near the surface. After the end of a pulse the heat quickly dissipates into the bulk of the material and a recast layer is formed [6].

The removal of material during laser milling is affected by the characteristics of the laser beam and the workpiece but is mainly determined by the way that both interact [2]. The wavelength, the

* Corresponding author. Tel.: +34 972 418265; fax: +34 972 418098.
E-mail addresses: daniel.teixidor@udg.edu (D. Teixidor), ines.iferrer@udg.edu (I. Ferrer), quim.ciurana@udg.edu (J. Ciurana), ozel@rci.rutgers.edu (T. Özel).

0736-5845/$ - see front matter © 2012 Elsevier Ltd. All rights reserved.
http://dx.doi.org/10.1016/j.rcim.2012.05.005

laser power, and pulse duration are the major factors that affect laser milling and can rarely be modified without changing the laser type with a few exceptions (e.g., Q-switching can provide the harmonics of the main wavelength). Laser ablation occurs only when the substrate material strongly absorbs the wavelength of the transmitted radiation. Hence, surface finishing, surface coating, and thermal conductivity are parameters which will lead to more or less effective laser milling. The process parameters that can be controlled and modified to obtain optimal machining results are the selection of the repetition rate of the pulses (frequency), the scanning speed, the hatch space, the hatch strategy, and the pulse intensity, all of which significantly affect the quality of the micro-feature created and the material removal rate.

Several research works deal with how process parameters affect the quality of the resultant surfaces or geometrical features using experimental analysis tools. Ciurana et al. [7] used a pulsed Nd:YAG laser to study the influence of pulse intensity, scanning speed, and pulse frequency on desired dimensions (angles, depth and width) and surface roughness in the laser micro-machining of hardened AISI H13 tool steel and they observed large variations in dimensional quality. Bartolo et al. [8] analyzed the influence of laser scanning strategies on surface roughness. Then, with the better strategy the influence of pulse frequency, laser power, and scanning speed on the material removal rate and surface roughness of tempered steel and aluminum was investigated. Their results suggest that lower pulse frequencies and laser power are more appropriate whenever surface quality is an issue. However, increasing both parameters is required until an optimum value for higher material removal rates are achieved. Cicala et al. [9] used an Nd:YAG pulsed laser for the machining of aluminum alloy, stainless steel, and titanium materials. They investigated the influence of the intensity, frequency, scanning speed, and line-spacing on the material removal rate and surface roughness. The results showed that the material removal rate depends mainly on the frequency of the laser pulses, and the surface roughness of the machined surface depends mainly on pulse frequency and, secondarily, on scanning speed. The lowest levels of roughness were obtained with the highest frequencies and with low scanning speeds. Campanelli et al. [10] had similar results analyzing the influence of pulse frequency, scanning strategy and overlapping on the depth of removed material and surface roughness in aluminum–magnesium alloy where the roughness results are generally contrary to the depth result. Kaldos et al. [11] studied the impact of the intensity, frequency and scanning speed on the surface roughness and material removal rate of die making steels. They used a CNC milling machine equipped with an Nd:YAG laser source as in the case of Quintana et al. [12], who conducted experiments with fixed parameters while machining aluminum, steel and titanium. Cheng et al. [13] analyzed the effects of pulse overlap, repetition rate and number of overscan on micro-processing quality and efficiency. They used femtosecond and picosecond lasers on copper, aluminum and titanium alloys. Kumar and Gupta [14] investigated the dependence of groove depth on laser power, repetition rate, number of scans and gas pressure in the generation of micro-notches in stainless steel and aluminum. Semaltianos et al. [15] studied the effects of the fluence and the pulse frequency on the MRR and the surface roughness in nickel based alloys with a Nd:IVO4 laser. They also analyzed the surface morphology with AFM and SEM techniques.

Some researchers have focused their interest on studying the pulse energy. Bordatchev and Nikumb [16] experimentally investigated the effect of it on the accuracy, precision and surface quality of copper machined parts. The results showed that the crater diameter and depth increase in accordance with the increase in the pulse energy. The use of lower pulse energy significantly improves the final accuracy and precision of machined parts, and reduces the process-affected zone, burrs, and damage to the surrounding material. Yousef et al. [17] investigated, analyzed, and modeled how the geometry of the crater (diameter, depth and volume of material removed) and final surface profile are formed and how they depend on the level of incident laser pulse energy. They used a diode pumped Nd:YAG laser and brass, copper and stainless steel as bulk material. Several other research works have focused on the interest in the pulse width (pulse duration). Chichkov et al. [18] presented experimental results on femtosecond, picosecond and nanosecond laser ablation of metal targets showing the advantage of femtosecond lasers over the others. Jandeleit et al. [19] studied the picosecond and nanosecond machining of gold, copper and some ceramics.

Finally, other research works developed models and methods to simulate the process and predict the results to assist in the design process. Ciurana et al. [7] developed multiple linear regression models and neural network models to predict surface roughness, and geometrical and dimensional features. In addition, the multi-objective particle swarm optimization (PSO) of process parameters of minimum surface roughness and minimum volume error was carried out. Petkov et al. [6] presented a method for analyzing the effects of pulse duration on surface integrity, surface roughness, and material microstructure changes. Dobrev et al. [20] developed a simulation model to investigate the influence of a number of laser ablation parameters on temperature distribution, heat flow, material removal and general laser–material interaction and the effects of crater profiles and laser milling strategies on resulting surface quality. Dhupal et al. [21] developed a mathematical model for the deviation of taper angle and depth deviation characteristics. Various tests modifying the air pressure, lamp current, pulse frequency, pulse width and scanning speed were carried out to serve as the bases of the model. Dhara et al. [22] developed a strategy for predicting the optimum machining parameter (air pressure, lamp current, pulse frequency and pulse width) settings for the generation of the maximum depth of groove with minimum height of recast layer. Bustillo et al. [23] presented research about the most appropriate modeling system for laser milling of copper components. The Box Jenkins (BJ) model was best adapted to this case, in terms of identifying the best conditions and predicting future circumstances.

This paper provides insight into optimizing process parameters to improve dimensional and surface quality in the laser milling micro-manufacturing process by optimizing process parameters. It is highly crucial to capture the influence of laser milling process parameters (e.g., scanning speed, laser pulse frequency and laser pulse intensity) on desired dimensional quality, geometrical feature size and surface finish. Moreover, it is also important to identify which ones have strong effects on the resultant quality of feature dimensions and surface while achieving target material removal rates and productivity. Therefore, this work will contribute to an understanding of the relations between process parameters and quality of the final geometrical features. The method used will also help develop a predictive system to identify the optimum set of process parameters considering different and possibly conflicting objectives. For this purpose, the multi-criteria based selection of laser milling process parameters for the most desired accuracy, geometry shape and surface finish is carried out using experimental models and the multi-objective particle swarm optimization (MOPSO) method.

1.1. Experimental work

The main objective of the experimental work was to investigate the influence of laser process parameters on dimensional precision and surface quality in laser milling of hardened AISI H13

Please cite this article as: Teixidor D, et al. Optimization of process parameters for pulsed laser milling of micro-channels on AISI H13 tool steel. Robotics and Computer Integrated Manufacturing (2012), http://dx.doi.org/10.1016/j.rcim.2012.05.005

tool steel and to evaluate the reliability and the availability of the process to produce micro-geometries instead of studying the productivity. The experiments were performed using a Deckel Maho Lasertec 40 machine, a nanosecond Nd:YAG lamp pumped solid-state laser, 100 W average laser power, and 1064 nm wavelength with a laser beam spot diameter of 0.03 mm. In the experiments the scanning speed (SS), the pulse frequency (PF), and the pulse intensity levels (PI) of a percentage of the ideal maximum pulse intensity were considered as a input process parameters.

In laser milling the incident laser beam is directed at the material to be removed. A focused, high-energy intensity spot area is created to ablate the material to be removed. Although the pulse intensity level on the surface was not measured during the experiments, an ideal pulse intensity level, based on the technical data of the laser system, can be given by

$$\mathrm{PI} = \frac{P}{\pi(d/2)^2} \tag{1}$$

where P is the laser power (100 W), and d is the beam spot diameter (0.03 mm). The ideal pulse intensity was estimated to be 141.4 kW/mm^2. Furthermore, the ideal peak pulse power (PPP) can be determined by

$$\mathrm{PPP} = \frac{P}{\tau} \tag{2}$$

where P is the laser power (100 W) and τ is the laser pulse duration (10 ns). For the laser characteristics used in this study, the peak pulse power is estimated to be 10 MW/s.

Fig. 1 represents a schematic 3D-laser milling process, where the rectangular cavity is machined by the motion of a laser beam in the x and y directions. The x, y and z axes were assumed to be along the width, length and depth, respectively, of the machined cavity. As shown in the figure, it was assumed that the volume of the cavity machined (corresponding to a certain depth in the z direction) per unit spot area by these physical phenomena was equivalent to a cylinder of diameter, d (beam diameter of 0.03 mm on surface of material being machined) [24,25]. Translation of the laser beam in the x and y directions led to material removal in all three directions (x, y and z) and a three-dimensional cavity was formed.

AISI H13 hardened tool steel was used in a workpiece material test. This material was selected because it is commonly used when mold inserts are needed. The experiments were carried out machining micro-channels of 200 μm in width and 50 μm in depth (Fig. 2).

Dimensional measurement was performed with a ZEISS SteREO Discovery.V12 stereomicroscope attached to DeltaPix digital camera of 3.75 MB for the collection of digital images with high resolution and contrast, and very good recording quality of texture and color. These images were numerically processed using the Quartz PCI© software, version 5.

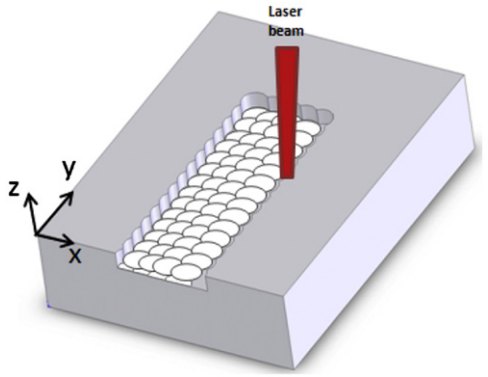

Fig. 1. Schematic illustration of three-dimensional laser milling process with pulse overlaps in the x and y directions and the cylindrical volume machined per spot area.

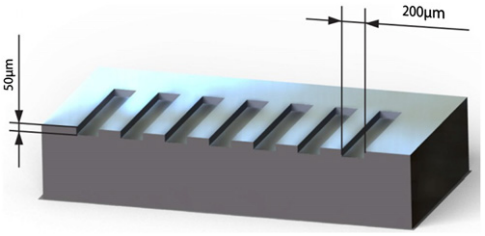

Fig. 2. Micro-channel design (not to scale).

Table 1
Factors and factor levels.

Factors	Factor levels		
Scanning speed (SS) (mm/s)	200	225	250
	275	300	325
	350	375	400
Pulse intensity (PI) (%)	35	40	45
Pulse frequency (PF) (kHz)	35	40	

The measurement of the surface roughness parameter R_a on the micro-channel bottom surface was conducted with a stylus instrument (Mitutoyo SV2000 Surftest equipment), with a cut off of 0.8 mm, in accordance to ISO/DIS 4287/1E. The R_a parameter was selected over other roughness parameters to study the surface roughness because it is used in several references and research studies. The ability of a profilometer to obtain the most precise and rapid surface measurements is affected by the reduced scale of the micro-channels. As a consequence, the profilometer stylus inside the micro-channel cannot be seen with the naked eye. In order to compensate for this difficulty, measurements were taken using a magnifying glass and intense illumination in the direction of the workpiece.

A full factorial design was used to determine the effects of pulse intensity, scanning speed, and pulse frequency on resultant dimensional precision and surface roughness in the laser milling of H13 hardened tool steel. The factors and factor levels are summarized in Table 1. These factor levels result in a total of 54 unique factor level combinations. The response variables are the surface roughness, R_a (μm) at the bottom of the micro-channel, micro-channel width dimension (μm), and micro-channel depth dimension (μm).

2. Experimental results

A total number of 54 micro-channels were machined with a laser machining process on a laser milling machine by following the experimental plan discussed in the previous section. The surface roughness was measured in five different sections of each micro-channel to obtain the mean value of the entire channel and the variation along its length. Then, each channel was cut in three parts to obtain the cross-sectional profiles where the measurements of depth and width were taken from the digital images processed using the software described previously. Again, five different measurements, proportionally distributed along the depth and the width, were taken. The mean (μ) and the standard deviation (σ) values of the experimental results obtained on the machined features for all the variable factor combinations are shown in Table 2.

Please cite this article as: Teixidor D, et al. Optimization of process parameters for pulsed laser milling of micro-channels on AISI H13 tool steel. Robotics and Computer Integrated Manufacturing (2012), http://dx.doi.org/10.1016/j.rcim.2012.05.005

Table 2
Experimental results.

Trial	PF (kHz)	PI (%)	SS (mm/s)	μDepth (μm)	σDepth (μm)	μWidth (μm)	σWidth (μm)	μR_a (μm)	σR_a (μm)	Time (s)
1	35	35	200	18.35	2.79	188.97	2.67	0.505	0.067	71
2	35	35	225	17.41	2.09	190.01	0.96	0.477	0.078	59
3	35	35	250	14.87	1.59	190.98	11.27	0.533	0.086	57
4	35	35	275	15.75	0.76	195.77	0.90	0.455	0.062	50
5	35	35	300	12.91	1.10	197.75	3.95	0.456	0.216	59
6	35	35	325	11.59	2.33	193.25	15.84	0.463	0.014	55
7	35	35	350	8.09	1.15	191.73	9.89	0.470	0.029	63
8	35	35	375	10.93	3.85	192.51	13.17	0.504	0.156	72
9	35	35	400	10.25	1.72	192.80	3.70	0.457	0.011	50
10	35	40	200	29.91	0.98	183.95	4.73	0.549	0.073	62
11	35	40	225	30.01	4.30	184.88	2.58	0.481	0.045	54
12	35	40	250	25.45	2.30	184.41	3.91	0.513	0.042	52
13	35	40	275	21.91	1.03	187.22	3.26	0.964	0.043	55
14	35	40	300	16.82	5.66	189.89	11.53	0.478	0.058	49
15	35	40	325	14.43	4.03	188.40	4.89	0.473	0.014	53
16	35	40	350	18.47	3.95	188.53	7.60	0.485	0.076	58
17	35	40	375	18.19	1.28	190.54	5.35	0.457	0.066	46
18	35	40	400	18.37	2.33	190.01	3.31	0.382	0.009	50
19	35	45	200	39.60	1.92	184.41	2.43	0.519	0.080	70
20	35	45	225	35.81	0.45	184.13	3.50	0.513	0.115	59
21	35	45	250	33.67	0.72	181.01	1.93	0.493	0.098	52
22	35	45	275	22.13	3.09	184.29	3.05	0.443	0.029	50
23	35	45	300	25.39	1.03	186.19	4.03	0.451	0.039	53
24	35	45	325	26.50	2.54	189.17	2.74	0.451	0.017	52
25	35	45	350	20.77	3.35	191.12	1.11	0.447	0.050	60
26	35	45	375	19.81	2.33	189.89	1.47	0.397	0.006	46
27	35	45	400	19.15	0.38	188.26	4.48	0.377	0.010	50
28	40	35	200	13.93	0.20	192.91	2.18	0.560	0.031	74
29	40	35	225	12.58	2.59	166.66	15.89	0.479	0.036	73
30	40	35	250	11.63	2.05	188.07	4.21	0.531	0.082	64
31	40	35	275	15.71	3.53	191.62	4.99	0.465	0.081	61
32	40	35	300	8.15	3.25	193.16	11.14	0.506	0.076	54
33	40	35	325	8.07	2.35	189.81	6.92	0.520	0.019	52
34	40	35	350	11.57	2.86	189.25	3.21	0.471	0.001	47
35	40	35	375	10.80	4.78	189.87	2.80	0.525	0.099	45
36	40	35	400	11.67	2.59	190.06	5.31	0.463	0.029	45
37	40	40	200	31.16	1.18	186.11	3.23	0.531	0.076	57
38	40	40	225	26.16	2.20	186.57	1.60	0.571	0.051	54
39	40	40	250	23.68	2.59	187.26	7.35	0.462	0.051	52
40	40	40	275	17.09	5.78	190.37	1.36	0.510	0.191	62
41	40	40	300	17.71	1.14	195.68	2.00	0.459	0.013	48
42	40	40	325	19.25	1.42	192.31	3.78	0.461	0.063	47
43	40	40	350	17.34	5.35	190.31	2.26	0.435	0.032	52
44	40	40	375	16.46	2.06	190.50	4.32	0.490	0.049	46
45	40	40	400	14.24	2.54	192.35	1.93	0.423	0.021	45
46	40	45	200	38.60	1.53	184.39	1.21	0.519	0.012	57
47	40	45	225	34.97	1.97	184.19	1.22	0.531	0.029	59
48	40	45	250	29.55	1.16	180.66	3.04	0.526	0.010	52
49	40	45	275	26.82	2.11	185.31	0.55	0.523	0.026	62
50	40	45	300	25.07	0.59	187.03	3.88	0.514	0.086	48
51	40	45	325	22.79	1.94	186.82	3.19	0.446	0.033	47
52	40	45	350	19.30	0.23	187.28	2.32	0.509	0.046	53
53	40	45	375	17.49	1.07	187.62	2.48	0.408	0.006	58
54	40	45	400	17.71	1.18	188.64	0.37	0.413	0.008	50

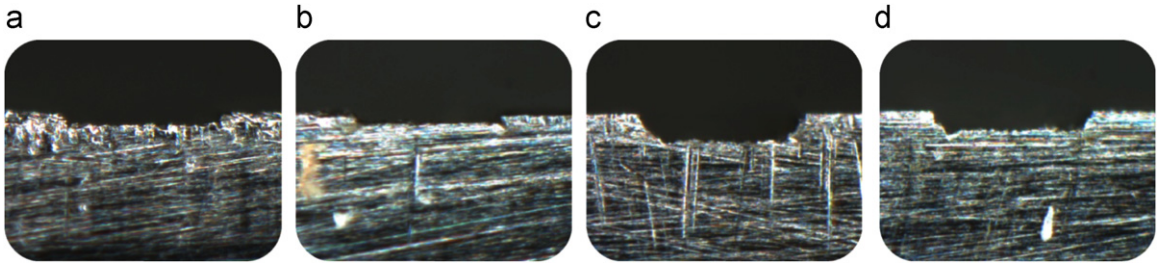

Fig. 3. Micro-channel images (200 ×): (a) scanning speed 275 mm/s, frequency 35 kHz and intensity 35% (Trial 4); (b) scanning speed 325 mm/s, frequency 35 kHz and intensity 40% (Trial 15); (c) scanning speed 225 mm/s, frequency 35 kHz and intensity 45% (Trial 20); and (d) scanning speed 300 mm/s, frequency 40 kHz and intensity 45% (Trial 50).

Please cite this article as: Teixidor D, et al. Optimization of process parameters for pulsed laser milling of micro-channels on AISI H13 tool steel. Robotics and Computer Integrated Manufacturing (2012), http://dx.doi.org/10.1016/j.rcim.2012.05.005

The dimensional and geometrical quality of the grooves produced with the laser milling process exhibit some variations as can be seen in Table 2. The target width or depth was never achieved in any of the experiments. It can also be seen that the deeper the channel, the worse the width. Fig. 3 presents some images of the profiles of the micro-channels produced using different laser input parameters. These images clearly indicate how irregular the laser milling process becomes when grooves with micro-features are manufactured.

These variations exhibit the complexity of the laser milling process and make clear the necessity of analyzing the data to find methods and models to select the best conditions and predict results to improve the productivity and the quality of the process.

The effect of scanning speed and pulse intensity parameters on the micro-channel depth is presented in Fig. 4, which shows that the closest depth value to the target was obtained with the lowest scanning speed and the highest pulse intensity combination. It is clear that the lower the scanning speed, the more time laser beam has to machine the surface and achieve higher depths. Pulse intensity plays an important role in the depth values. Higher pulse intensities produce deeper grooves with each laser beam pass. The pulse frequency does not seem to affect the depth value.

Fig. 5 shows the effect of scanning speed and pulse intensity on the micro-channel width. In this case, unlike in that of depth, the experimental values are closer to the target width (0.2 mm) when the scanning speed is high and the pulse intensity is low. These opposite effects on the depth and the width are due to straight walls being really difficult to achieve. Thus, when the channel becomes deeper, the width becomes narrower, and a smaller mean width value is obtained. Also, the higher the pulse frequency is, the higher the micro-channel width becomes.

The effect of the scanning speed and the pulse intensity on the surface roughness is less clear than in the previous cases (Fig. 6). The best surface roughness values were obtained by a combination of the highest pulse intensity and the highest scanning speed. The influence of scanning speed on surface roughness in laser micro-machining processes can be explained as follows: the laser beam may not affect the surface roughness as much when movement is fast, but when movement is slow surface roughness does not improve. However, the experimental values do not show so many differences due to the range vary between 0.4 and 0.55 μm. The level of pulse frequency does not have too much effect on the surface roughness.

Figs. 4–6 illustrate the trends in effects of process parameters on the dimensional and geometrical quality of a micro-channel feature; however, these offer no prediction capability, and it is hard to use them directly in process planning without using an intelligent computational tool. Therefore, second order models

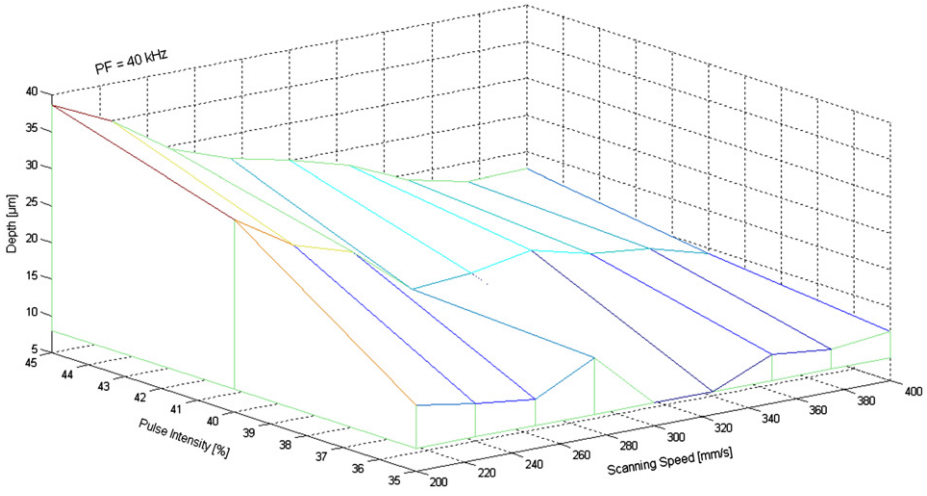

Fig. 4. Effect of pulse intensity and scanning speed on micro-channel depth (PF = 40 kHz).

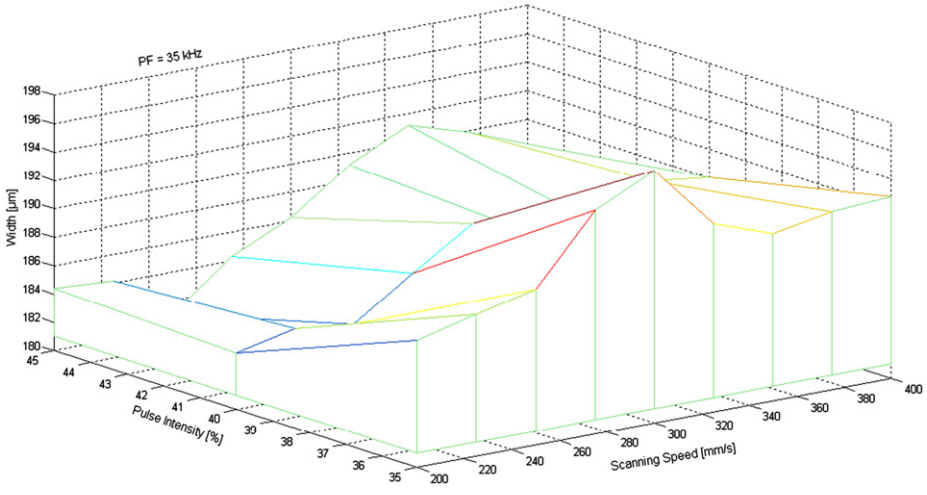

Fig. 5. Effect of the scanning speed and pulse intensity on the micro-channel width (PF = 35 kHz).

Please cite this article as: Teixidor D, et al. Optimization of process parameters for pulsed laser milling of micro-channels on AISI H13 tool steel. Robotics and Computer Integrated Manufacturing (2012), http://dx.doi.org/10.1016/j.rcim.2012.05.005

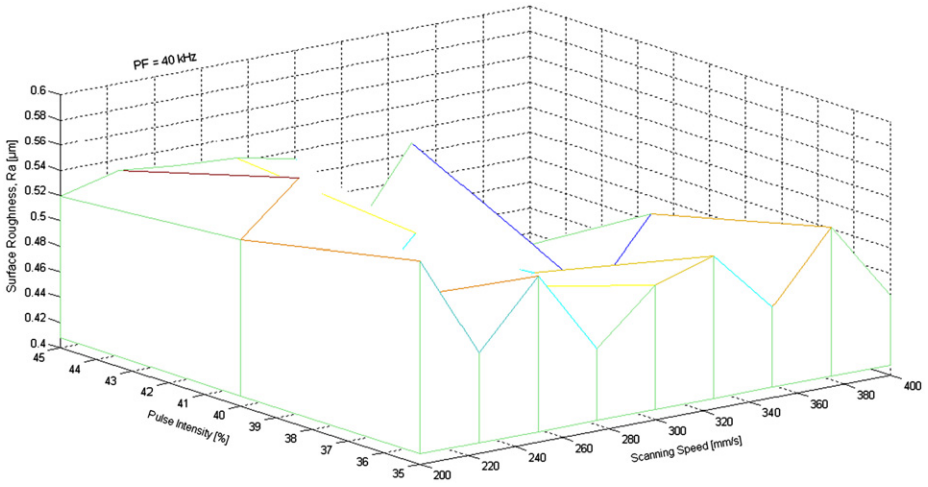

Fig. 6. Effect of scanning speed and pulse intensity on surface roughness (PF = 40 kHz).

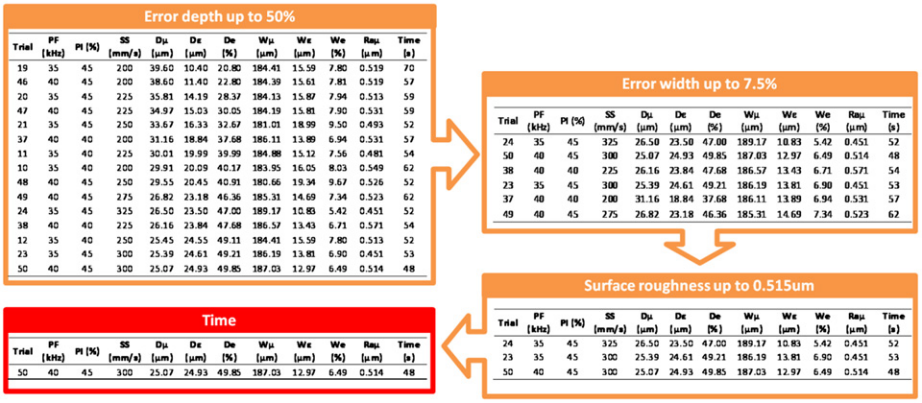

Fig. 7. Example of the multi-criteria selection process for the εDepth (up to 50%) → εWidth (up to 7.5%) → R_a (up to 0.515 μm) → time.

Table 3
Best combinations for the multi-criteria selections.

Multi-criteria selection	Trial	PF (kHz)	PI (%)	SS (mm/s)
εDepth (up to 50%) → εWidth (up to 7.5%) → R_a (up to 0.515 μm) → time	50	40	45	300
εWidth (up to 5%) → εDepth (up to 70%) → R_a (up to 0.460 μm) → time	17	35	40	375
R_a (up to 0.450 μm) → εDepth (up to 50%) → εWidth	25	35	45	350
R_a (up to 0.450 μm) → εWidth (up to 5%) → εDepth	25	35	45	350
εDepth (up to 50%) → εWidth (up to 7.8%) → σDepth (up to 2.0 μm) → σWidth	19	35	45	200
εWidth (up to 5%) → εDepth (up to 70%) → σWidth (up to 4.0 μm) → σDepth	4	35	35	275
R_a (up to 0.460 μm) → εDepth (up to 65%) → εWidth (up to 5.5%) → σDepth (up to 2.5 μm) → σWidth	26	35	45	375
R_a (up to 0.460 μm) → εWidth (up to 5.0%) → εDepth (up to 70%) → σWidth (up to 10.0 μm) → σDepth	4	35	35	275

and PSO are employed to establish this input and output relationship and predict the optimal process parameters. Also, a multi-criteria selection method is used to find the best combinations for different quality criteria.

2.1. Multi-criteria ranking and selection of process parameters

In this paper, a multi-criteria selection method is presented to establish the initial process parameters, which depend on the preferences of the final part characteristics. The method consists in filtering, step by step, the data obtained from the experimental design with established, prioritized criteria, in order to obtain the best process characteristic combinations that result in the desired quality. With this method it is possible to achieve acceptable, quality results for multiple characteristics. The user can establish quality ranges for each output parameter and the combinations that are out of the range are eliminated step by step. So, in the end, the best combination for the criteria is the order selected.

Fig. 7 shows an example of the method/process. In this example the first criterion selected is the depth, and the data is filtered by the depth error percentage up to 50% to reduce the number of combinations to 15. This error range is wide because the results obtained for the depth value were not close to the target. The second criterion selected is the width, and the data is filtered by the width error percentage up to 7.5% to reduce the combinations to six. The third criterion is the surface roughness. In this case there was not a target value, so the data is filtered by the R_a value, establishing the limit at 0.515 μm. Table 4 shows the three remaining combinations. Finally, the last criterion used is the processing time that achieves the best process parameter

Please cite this article as: Teixidor D, et al. Optimization of process parameters for pulsed laser milling of micro-channels on AISI H13 tool steel. Robotics and Computer Integrated Manufacturing (2012), http://dx.doi.org/10.1016/j.rcim.2012.05.005

Table 4
Model parameters for the response in laser milling of steel.

Coef.	Dμ (μm)	Dσ (μm)	Wμ (μm)	Wσ (μm)	$R_a\mu$ (μm)	$R_a\sigma$ (μm)
Constant	19.30637646	3.09113497	188.65224788	4.99182540	0.48098498	0.04922962
PI	6.96888888	−0.38953735	−2.29170543	−2.11066182	−0.01006574	−0.00476403
PF	−0.68629629	0.02153868	0.15773619	−0.58382381	0.00998468	−0.00322906
SS	−6.82014814	0.28046390	2.20940114	0.38492483	−0.04482011	−0.01912820
PF^2	–	–	–	–	–	–
PI^2	−1.49740740	−0.86221603	−0.44302666	0.33583218	0.00089479	−0.00236796
SS^2	3.88425204	−0.73581535	−1.35701459	−1.98547325	−0.00201368	−0.00774625
PI · PF	0.15296296	−0.30101644	0.13044464	−0.02282023	0.00272870	−0.00624486
PI · SS	−3.66911111	−0.33677867	1.28780939	−0.40730512	−0.02269138	−0.00197180
PF · SS	0.37659259	0.09088012	−0.79816099	−1.05231278	0.0004567	0.01242588
R-sq	94.17%	25.89%	74.73%	33.39%	62.47%	33.26%
R-sq (adj)	93.13%	12.71%	69.67%	21.55%	55.65%	20.54%

combination for this specific multi-criterion. The ranges of the different criteria are selected to reduce the number of combinations. With the first criterion the goal is to reduce the 54 experiments into 10–15 combinations, a number that will provide enough data. Then, in the following steps, the idea is to filter this first group in smaller parts until the last criterion when just one combination is selected.

Table 3 shows the best combination for the different multi-criteria selections used. As can be seen, there is not one combination that fulfils all the criteria. These results make clear that laser milling is a complex process and is not easy to find the proper combination of process parameters to achieve different quality outputs. With this multi-criteria selection method the user can find the best combination of criteria used to obtain results between established quality ranges.

2.2. Experimental modeling

In this study, a second order model is used to efficiently establish input–output relationships between response and controllable variables that takes the generic form

$$y = \beta_0 + \sum_{i=1}^{k} \beta_i x_i + \sum_{i=1}^{k} \beta_{ij} x_i x_j + \sum_{i=1}^{k} \beta_{ii} x_i^2 + \varepsilon \tag{3}$$

where ε is the residual error.

Experimental models were developed using the generic regression form in Eq. (3) for responses of depth (μm), width (μm) and surface roughness R_a (μm) for the mean (μ) and the standard deviation (σ) values using the experimental test data and establishing the effect of variables on the outputs.

Since the analysis was done with coded values, the codification of the control parameters can be calculated with Eqs. (4)–(6) where PI is the pulse intensity (%), PF is the pulse frequency (kHz) and SS is the scanning speed (mm/s)

$$A = \frac{\mathrm{PI}-40}{5} \tag{4}$$

$$B = \frac{\mathrm{PF}-37.5}{2.5} \tag{5}$$

$$C = \frac{\mathrm{SS}-300}{100} \tag{6}$$

The six responses can be related with the three controllable process variables, $x_1 = \mathrm{PI}$, $x_2 = \mathrm{PF}$, $x_3 = \mathrm{SS}$, including the interaction terms and the second order terms as follows:

$$\mu\mathrm{Depth} = \beta_0 + \beta_1\mathrm{PI} + \beta_2\mathrm{PF} + \beta_3\mathrm{SS} + \beta_{12}\mathrm{PI}\cdot\mathrm{PF} + \beta_{13}\mathrm{PI}\cdot\mathrm{SS} + \beta_{23}\mathrm{PF}\cdot\mathrm{SS} + \beta_{11}\mathrm{PI}^2 + \beta_{33}\mathrm{SS}^2 + \varepsilon \tag{7}$$

$$\sigma\mathrm{Depth} = \beta_0 + \beta_1\mathrm{PI} + \beta_2\mathrm{PF} + \beta_3\mathrm{SS} + \beta_{12}\mathrm{PI}\cdot\mathrm{PF} + \beta_{13}\mathrm{PI}\cdot\mathrm{SS} + \beta_{23}\mathrm{PF}\cdot\mathrm{SS} + \beta_{11}\mathrm{PI}^2 + \beta_{33}\mathrm{SS}^2 + \varepsilon \tag{8}$$

$$\mu\mathrm{Width} = \beta_0 + \beta_1\mathrm{PI} + \beta_2\mathrm{PF} + \beta_3\mathrm{SS} + \beta_{12}\mathrm{PI}\cdot\mathrm{PF} + \beta_{13}\mathrm{PI}\cdot\mathrm{SS} + \beta_{23}\mathrm{PF}\cdot\mathrm{SS} + \beta_{11}\mathrm{PI}^2 + \beta_{33}\mathrm{SS}^2 + \varepsilon \tag{9}$$

$$\sigma\mathrm{Width} = \beta_0 + \beta_1\mathrm{PI} + \beta_2\mathrm{PF} + \beta_3\mathrm{SS} + \beta_{12}\mathrm{PI}\cdot\mathrm{PF} + \beta_{13}\mathrm{PI}\cdot\mathrm{SS} + \beta_{23}\mathrm{PF}\cdot\mathrm{SS} + \beta_{11}\mathrm{PI}^2 + \beta_{33}\mathrm{SS}^2 + \varepsilon \tag{10}$$

$$\mu R_a = \beta_0 + \beta_1\mathrm{PI} + \beta_2\mathrm{PF} + \beta_3\mathrm{SS} + \beta_{12}\mathrm{PI}\cdot\mathrm{PF} + \beta_{13}\mathrm{PI}\cdot\mathrm{SS} + \beta_{23}\mathrm{PF}\cdot\mathrm{SS} + \beta_{11}\mathrm{PI}^2 + \beta_{33}\mathrm{SS}^2 + \varepsilon \tag{11}$$

$$\sigma R_a = \beta_0 + \beta_1\mathrm{PI} + \beta_2\mathrm{PF} + \beta_3\mathrm{SS} + \beta_{12}\mathrm{PI}\cdot\mathrm{PF} + \beta_{13}\mathrm{PI}\cdot\mathrm{SS} + \beta_{23}\mathrm{PF}\cdot\mathrm{SS} + \beta_{11}\mathrm{PI}^2 + \beta_{33}\mathrm{SS}^2 + \varepsilon \tag{12}$$

The second-order terms of the process variable PF is not presented because only two levels were used and it was not possible to use this term for the estimation. The statistical analysis resulted in the estimated experimental model parameters as given in Table 4.

2.3. Multi-objective particle swarm optimization (MOPSO)

Multi-objective optimization problems can be solved using evolutionary computational algorithms such as genetic algorithms and particle swarm optimization [26]. We conducted multi-criteria optimization to investigate the dimensional and geometrical accuracy in laser milling of hardened tool steel for micro-channel fabrication on medical devices. The optimal selection of laser milling process parameters can be formulated and solved as an optimization problem. The experimental results obtained in this work indicate that the laser milling of micro-channels requires simultaneous consideration of multiple objectives, including achieving the target depth and width (minimum error) and a minimum surface roughness. Usually, the process parameters selected for one objective function are not suitable for the other objective function, creating conflicting objectives. This presents a challenge for the optimization problem, since the parameter settings (decision variables) selected for given multiple choices may be in conflict with each other. For this purpose the two objective functions are considered separately:

$$\text{minimize}\{f(x), g(x), h(x)\}$$

$$\text{s.t.} \quad f(x) \le b_1 \text{ and } g(x) \le b_2 \text{ and } h(x) \le b_2 \text{ where } x \in X \tag{13}$$

In the optimization problem formulation in Eq. (13) $f(x)$, $g(x)$, $h(x)$ represent the objective functions for depth error, width error, and surface roughness, respectively, with a set of process parameters ($x = x_1 + \cdots + x_n$, $n = 1,2$ or 3). X is the solution space with all feasible values for the process parameters.

Please cite this article as: Teixidor D, et al. Optimization of process parameters for pulsed laser milling of micro-channels on AISI H13 tool steel. Robotics and Computer Integrated Manufacturing (2012), http://dx.doi.org/10.1016/j.rcim.2012.05.005

In the formulation given above, the objective is to simultaneously minimize the objective functions. In solving this optimization problem, a general approach based on a Pareto-optimal set of non-dominated decision variable settings is considered. The selection of a Pareto-optimal set avoids the problem of a single combined objective function with weights, which often leads to a unique solution but offers no other solution for optimum parameter selection to the decision maker.

In the case of a laser milling process, the optimization problem is defined with multiple objectives. Decision variables such as scanning speed (SS), pulse intensity (PI) and pulse frequency (PF) are constrained within the ranges of the experiments (see Table 3).

The multi-objective optimization problem has been solved using the dynamic neighborhood-particle swarm optimization (DN-PSO) method proposed by Hu and Eberhart [27]. In DN-PSO, several neighborhoods are defined for each particle and local *optimums* are found within these neighborhoods. If a two-dimensional objective function space in a *min–min* problem is considered, the Pareto front is the boundary of the objective value region, which is the lower left side of the objective function space for *min–min* problems. The objective of the proposed algorithm is to drop those solutions onto the boundary line indicated by a solid line. For this purpose, the first objective function is fixed to define neighborhoods and the second objective function is used in optimization. According to the DN-PSO algorithm; (1) the distances between the current particle and other particles are calculated in terms of the first objective function, (2) based on these distances, the nearest m (neighborhood size) particles are found, and (3) the local best particle among neighbors is selected in terms of the second objective function. In order to handle constraints, a simple modification to the particle swarm optimization algorithm is sufficient. The DN-PSO optimization algorithm combined with constraints was converted into a code using *Matlab* software. This MOPSO procedure using the DN-PSO method is explained in detail in previous works [28–30].

The simulations are run using a population of 200 for the particle swarm and a maximum number of 300 iterations. After obtaining the best particle values in each iteration of the simulation, the particles are plotted in a two-dimensional objective space for viewing. This procedure is repeated until a clear Pareto frontier forms. Then, the Pareto frontiers of the non-dominated solution sets are obtained using multi-objective PSO method as shown in Figs. 8–10.

This dimensional accuracy must be the first criteria when micro-channel fabrication for micro-medical devices is the objective. So, the multi-objective optimization of the depth and width errors (Fig. 8) must be analyzed before the surface roughness

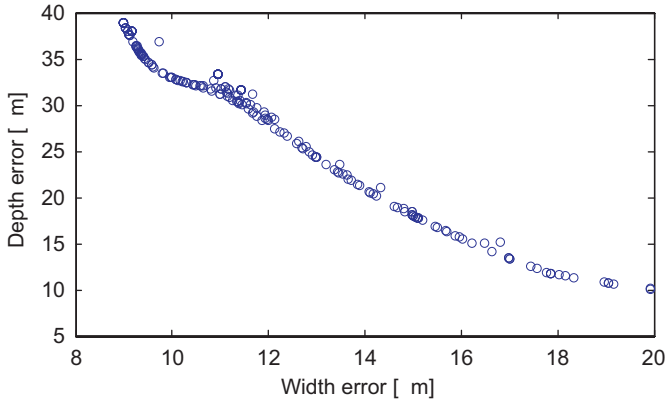

Fig. 8. Pareto frontier of optimal depth and width errors of laser milling parameters.

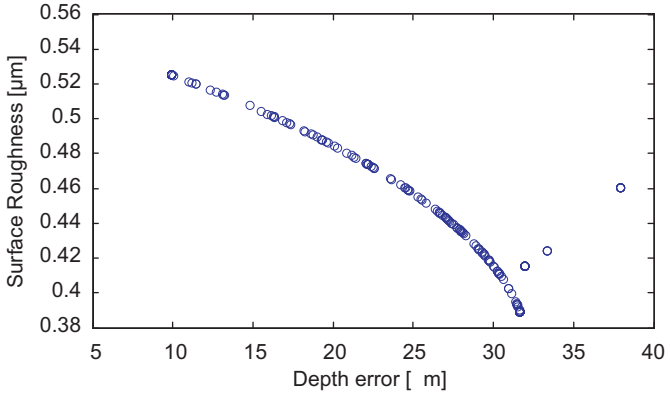

Fig. 9. Pareto frontier of optimal surface roughness and depth error of laser milling parameters.

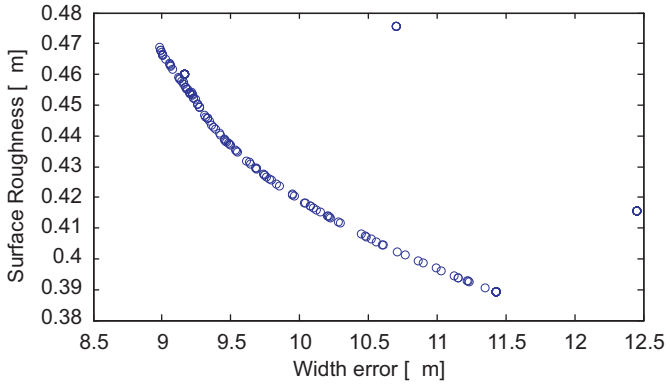

Fig. 10. Pareto frontier of optimal surface roughness and width error of laser milling parameters.

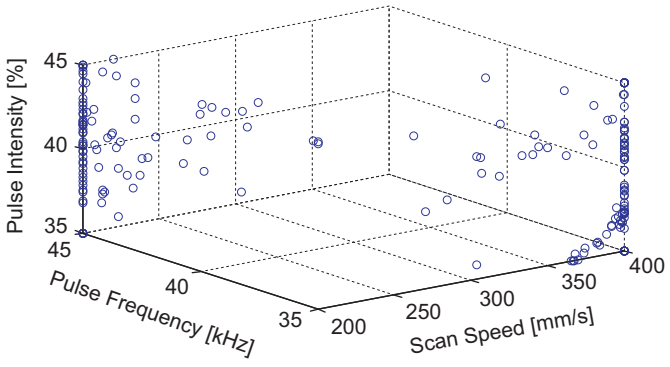

Fig. 11. Decision variable space for optimal laser milling parameters for depth and width.

analysis. As the previous results have shown, there is no optimum parameter condition that can achieve the target value of depth or width. The minimum depth error is close to 10 μm, with a corresponding width error of 20 μm, and the other combinations of parameters will result in better width but higher depth error. The little convexity in the axes bisector line confirms that both objective parameters are unrelated.

The convexity shape of the Pareto frontier in Fig. 9 shows a clear independence between the surface roughness and depth error objective parameters. A lower surface roughness will result in a higher depth dimensional error. The lowest depth error is around 10 μm with a surface roughness of 0.53 μm. However, the

Please cite this article as: Teixidor D, et al. Optimization of process parameters for pulsed laser milling of micro-channels on AISI H13 tool steel. Robotics and Computer Integrated Manufacturing (2012), http://dx.doi.org/10.1016/j.rcim.2012.05.005

Pareto frontier of optimal surface roughness and width error (Fig. 10) presents a concave shape, indicating that it is possible to improve both surface roughness and width error by changing some conditions.

As a result of these investigations, it can be claimed that none of the combinations reaches an optimal result. That could be because the range of levels selected for some of the input parameters is not wide enough to obtain the optimum. No combination exceeds the target values of depth and width so the range levels of pulse intensity and pulse frequency must be wide to get these kinds of outputs. Furthermore, non-dominated optimal solutions that form the Pareto front in objective function space are analyzed in decision variable space ($x_1 = \text{SS}, x_2 = \text{PI}$ and $x_3 = \text{PF}$) as shown in Figs. 11–13.

The particles (circles in the figures) representing the optimal set of decision variables for depth and width errors given in Fig. 8 are mapped into the decision variable space as shown in Fig. 11.

As can be seen from this figure, the optimal laser milling parameters occur along the boundaries of the decision variable space, i.e., around a pulse frequency (PF) of 45 kHz and a scanning speed (SS) of 400 mm/min. This tends to confirm that the range levels of the parameters selected could be wider. The particles try to reach high values for pulse frequency and scanning speed to get better results for the depth and width of the micro-channel.

Similarly, the optimal decision variables for laser milling for optimization of surface roughness and depth error are mapped from objective space in Fig. 9 into the decision variable space as shown in Fig. 12. In that case the optimal parameters are not aligned along the boundaries of the decision variable space, and the particles are diagonally descending from one vertex with high pulse intensity and scanning speed and low pulse frequency to a medium point in the decision variable space.

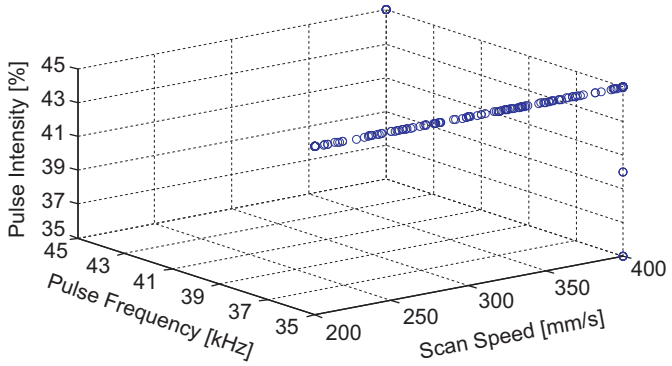

Fig. 12. Decision variable space for optimal laser milling parameters for depth and surface roughness.

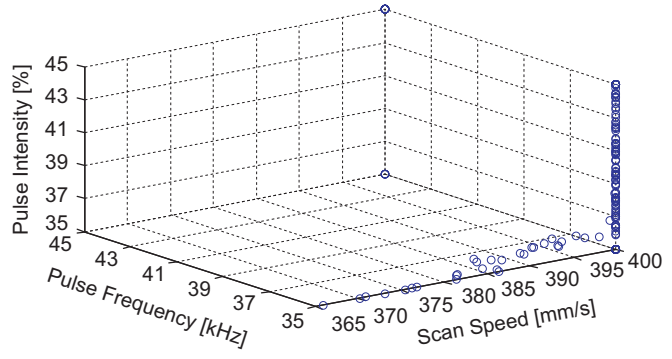

Fig. 13. Decision variable space for optimal laser milling parameters for depth and width.

Finally, the optimal decision variables for laser milling for optimization of surface roughness and width error are mapped from objective space in Fig. 10 into the decision variable space as shown in Fig. 13. In that case the optimal parameters are firmly aligned along the scanning speed boundary of 40 mm/s and close to the pulse frequency boundary of 35 kHz, showing that the highest scanning speed values would lead to better results and get closer to optimum surface roughness and width values. In addition, the low pulse frequencies make the results better.

3. Conclusions

In this study, surface finishing and dimensional features of micro-channels have been investigated in laser milling process of hardened AISI H13 tool steel. 3D plots are used to illustrate the trends of the effects of the process parameters and a method using multi-criteria ranking and selection of parameters is presented to find the best combinations for different quality criteria. Experimental models based on quadratic regression are developed for surface roughness and width and depth errors. Furthermore, an evolutionary computational approach is applied to the decision-making problem in micro-machining parameters. Finally, an analysis of optimal solutions that form the Pareto front in objective function space is provided in decision variable space. The analysis indicates that the control parameter level ranges should be wider to obtain results close to the optimum. However, some trends and specific conclusions can be drawn:

1. Although the dimensions and shape of the micro-channels produced with laser micro-milling processes exhibit variations, the results suggest that laser machining is a process capable of producing micro-geometries.
2. Laser milling is a complex process and it is not easy to find the proper combination of process parameters to achieve different quality outputs.
3. A multi-criteria ranking and parameter selection method can find the best combination of those used to obtain results between established quality ranges.
4. A multi-objective particle swarm optimizer provides Pareto frontiers of non-dominated solution sets for optimum laser milling process parameters, providing decision makers with a resourceful and efficient means of achieving it.
5. Analyses of optimal solutions in decision variable space show that the particular optimal micro-milling parameters are along the boundaries of the objective function space.

Acknowledgments

The authors would like to express their gratitude to the GREP research group from the UdG, the MARL group at Rutgers University, and the ASCAMM Technology Center for the facilities provided during the experiments. This work was partially carried out with the grant supports from the European Commission project IREBID (FP7-PEOPLE-2009-IRSES-247476) and the Spanish Science and Innovation Minister project TECNIPLAD (DPI2009-09852).

References

[1] Dubey AK, Yadava V. Laser beam machining—a review. International Journal of Machine Tools and Manufacture 2008;5;48(6):609–628.
[2] Pham DT, Dimov SS, Petkov PV. Laser milling of ceramic components. International Journal of Machine Tools and Manufacture 2007;3;47(3-4): 618–626.

[3] Pham DT, Dimov SS, Ji C, Petkov PV, Dobrev T. Laser milling as a 'rapid micromanufacturing process. Proceedings of the Institution of Mechanical Engineer Part B: Journal of Engineering Manufacture 2004;218(1):1–7.
[4] Uriarte L, Herrero A, Ivanov A, Oosterling H, Staemmler L, Tang PT, et al. Comparison between microfabrication technologies for metal tooling. Proceedings of the Institution of Mechanical Engineer Part C 2006;220(11):1665–1676.
[5] Dubey AK, Yadava V. Experimental study of Nd:YAG laser beam machining—an overview. Journal of Materials Processing Technology 2008;195(1–3): 15–26.
[6] Petkov PV, Dimov SS, Minev RM, Pham DT. Laser milling: pulse duration effects on surface integrity. Proceedings of the Institution of Mechanical Engineer Part B: Journal of Engineering Manufacture 2008;222(1):35–45.
[7] Ciurana J, Arias G, Ozel T. Neural network modeling and particle swarm optimization (PSO) of process parameters in pulsed laser micromachining of hardened AISI H13 steel. Materials and Manufacturing Processes 2009;24(3):358–368.
[8] Bartolo P, Vasco J, Silva B, Galo C. Laser micromachining for mould manufacturing: I. The influence of operating parameters. Assembly Automation 2006;26(3):227–234.
[9] Cicală E, Soveja A, Sallamand P, Grevey D, Jouvard JM. The application of the random balance method in laser machining of metals. Journal of Materials Processing Technology 2008;196(1–3):393–401.
[10] Campanelli SL, Ludovico AD, Bonserio C, Cavalluzzi P, Cinquepalmi M. Experimental analysis of the laser milling process parameters. Journal of Materials Processing Technology 2007;191(1–3):220–223.
[11] Kaldos A, Pieper HJ, Wolf E, Krause M. Laser machining in die making—a modern rapid tooling process. Journal of Materials Processing Technology 2004;155–156:1815–1820.
[12] Quintana I, Etxarri J, Sanz C, Aranzabe A. Laser micro-milling and drilling using microsecond pulses. Applications for mould and aeronautical industry. In: ICMEN 2008 3rd international conference of manufacturing engineering; 2008. p. 167–4.
[13] Cheng J, Perrie W, Edwardson SP, Fearon E, Dearden G, Watkins KG. Effects of laser operating parameters on metals micromachining with ultrafast lasers. Applied Surface Science 2009;256(5):1514–1520.
[14] Kumar A, Gupta MC. Laser machining of micro-notches for fatigue life. Optics and Lasers in Engineering 2010;48(6):690–697.
[15] Semaltianos NG, Perrie W, Cheng J, French P, Sharp M, Dearden G, et al. Picosecond laser ablation of nickel-based superalloy C263. Applied Physics A: Materials Science and Processing 2010;98(2):345–355.
[16] Bordatchev EV, Nikumb SK. An experimental study and statistical analysis of the effect of laser pulse energy on the geometric quality during laser precision machining. Machining Science and Technology 2003;7(1):83–104.
[17] Yousef BF, Knopf GK, Bordatchev EV, Nikumb SK. Neural network modeling and analysis of the material removal process during laser machining. International Journal of Advanced Manufacturing Technology 2003;22(1-2):41–53.
[18] Chichkov BL, Momma C, Nolte S, Von Alvens leben F, Tünnermann A. Femtosecond, picosecond and nanosecond laser ablation of solids. Applied Physics A 1996;63:109–115.
[19] Jandeleit J, Horn A, Weichenhain R, Kreutz EW, Poprawe R. Fundamental investigations of micromachining by nano- and picosecond laser radiation. Applied Surface Science 1998;127–129:885–891.
[20] Dobrev T, Dimov SS, Thomas AJ. Laser milling: modelling crater and surface formation. Proceedings of the Institution of Mechanical Engineer Part C 2006;220(11):1685–1696.
[21] Dhupal D, Doloi B, Bhattacharyya B. Parametric analysis and optimization of Nd:YAG laser micro-grooving of aluminum titanate (Al_2TiO_5) ceramics. International Journal of Advanced Manufacturing Technology 2008;36(9–10):883–893.
[22] Dhara SK, Kuar AS, Mitra S. An artificial neural network approach on parametric optimization of laser micro-machining of die-steel. International Journal of Advanced Manufacturing Technology 2008;39(1-2):39–46.
[23] Bustillo A, Sedano J, Villar J, Curiel L, Corchado E. AI for modelling the laser milling of copper components. In: Fyfe C, Kim D, Lee S, Yin H, editors. Berlin/ Heidelberg: Springer; 2008. p. 498.
[24] Samant AN, Dahotre NB. Three-dimensional laser machining of structural ceramics. Journal of Manufacturing Processes 2010;12(1):1–7.
[25] Samant AN, Dahotre NB. An integrated computational approach to single-dimensional laser machining of magnesia. Optics and Lasers in Engineering 2009;5;47(5):570–577.
[26] Coello Coello CA, Becerra RL. Evolutionary multiobjective optimization in materials science and engineering. Materials and Manufacturing Processes 2009;24(2):119–129.
[27] Hu X, Eberhart R. Multiobjective optimization using dynamic neighborhood particle swarm optimization. In: Proceedings of IEEE swarm intelligence symposium; 2002. p. 1404–11.
[28] Karpat Y, Özel T. Multi-objective optimization for turning processes using neural network modeling and dynamic-neighborhood particle swarm optimization. The International Journal of Advanced Manufacturing Technology 2007;35(3–4):234–247.
[29] Ciurana J, Arias G, Ozel T. Neural network modeling and particle swarm optimization (PSO) of process parameters in pulsed laser micromachining of hardened AISI H13 steel. Materials and Manufacturing Processes 2009;24(3): 358–368.
[30] Vázquez E, Ciurana J, Rodríguez CA, Thepsonthi T, Özel T. Swarm intelligent selection and optimization of machining system parameters for microchannel fabrication in medical devices. Materials and Manufacturing Processes 2011;26(3):403–414.

Please cite this article as: Teixidor D, et al. Optimization of process parameters for pulsed laser milling of micro-channels on AISI H13 tool steel. Robotics and Computer Integrated Manufacturing (2012), http://dx.doi.org/10.1016/j.rcim.2012.05.005